

DYNAMIC ANALYSIS OF PLATES WITH CUT-OUT CARRYING CONCENTRATED AND DISTRIBUTED MASS

(DOI No: 10.3940/rina.ijme.2020.a3.612)

S Pal and **S Haldar**, Indian Institute of Engineering Science and Technology, India, **K Kalita**, Vel Tech Rangarajan Dr. Sagunthala R&D Institute of Science and Technology, India

KEY DATES: Submitted: 26/12/19; Final acceptance: 28/08/20; Published: 07/10/20

SUMMARY

An isoparametric plate bending element with nine nodes is used in this paper for dynamic analysis of isotropic cut-out plate having concentrated and uniformly distributed mass on the plate. The Mindlin's first-order shear deformation theory (FSDT) is used in the present finite element formulation. Two proportionate mass lumping schemes are used. The effect of rotary inertia is included in one of the mass lumping schemes in the present element formulation. Dynamic analysis of rectangular isotropic plates with cut-out having different side ratio, thickness ratio and boundary condition is analysed using a finite element method. The present results are compared with the published results. Some new results on isotropic plates with cut-out having different side ratio, ratio of side-to-thickness of the plate, different position and size of cut-out in plates subjected to transversely concentrated and distributed mass are presented.

NOMENCLATURE

[B]	Strain-displacement matrix
[D]	Rigidity matrix
[K]	Global stiffness matrix
[N]	Shape function
[M]	Consistent mass matrix
J	Jacobian matrix
[N _r]	Interpolation function of the r th point
[K ₀]	Overall stiffness matrix
[M ₀]	Overall Mass matrix
u, v	In-plane displacement
w	Transverse displacement
E	Modulus of elasticity
G	Modulus of rigidity
ν	Poisson's ratio
h	Thickness of plate
a, b	Plate dimensions
D	Flexural rigidity
ω	Natural frequency
θ _x θ _y	Total rotation in bending
{σ}	Stress vector
{ε}	Strain vector
M _x , M _y	Bending moments in x and y-direction
M _{xy}	Twisting moment
Q _x Q _y	Transverse shear forces
ξ, η	Natural coordinates
ρ	Density
HBM	Hencky bar-net model
FEM	Finite element method
FSDT	First-order shear deformation theory
HSDT	Higher order shear deformation theory
TSDT	Third-order shear deformation theory

due to large oscillations are essential for the design of the aircraft wings and watercraft casing. Cut-out plates are used for lift passage on a floor and window in aircraft etc. Also, plates with different attachment are used in engineering application.

The literature on free vibration of isotropic plates is vast. Here only a few important papers are discussed which is related to the present work. Zhang et al. (Zhang, Wang, Pedroso, & Zhang, 2018) studied vibration analysis of a rectangular plate with rectangular cut-out using the Hencky bar-net model (HBM). They extended Hencky bar-net model considering rotationally elastic and transverse spring stiffnesses at the cut-out corners. They presented non-dimensional frequency parameters for cut-out plates and also for cracked corner cut-out plates with different boundary conditions. Influence of rotary and shear on flexural motions of isotropic elastic plate was examined by Mindlin (Mindlin, 1951), and he presented closed-form solution of isotropic plate. Vibration analysis of cut-out plates using a modified Rayleigh-Ritz method was investigated by Lam et al. (Lam, Hung, & Chow, 1989). They divided the plate into a rectangular segment and subtracted elements which are in cut-out location to obtain the cut-out plate. They presented non-dimensional frequencies for the cut-out isotropic and orthotropic plates and compared with the previously published literature. Abbas et al. (Abbas, Abdullah, & Wasmi, 2015) presented static and free vibration of a thin plate using finite element analysis (FEA). For the finite element analysis, they used ANSYS finite element software. Manna (Manna, 2005) studied free vibration analysis of isotropic rectangular plate. He used a higher-order triangular finite element having 18 nodes on the side and 6 internal nodes and also considered first-order shear deformation theory (FSDT). He presented a variation of non-dimensional frequency in different thickness ratio, aspect ratio, and boundary conditions. Kalita and Haldar (Kalita & Haldar, 2016) investigated free vibration of rectangular central cut-out plates using a 9-node isoparametric plate element for the finite element

1. INTRODUCTION

Plates with cut-out are generally used in civil, mechanical, aerospace and marine structures. In aerospace and marine industry generally, thin plates are used. Effect on plates

formulation. Park and Choi (Park & Choi, 2018) considered Mindlin's theory for free vibration analysis of isotropic plates. Free vibration of rectangular cut-out plates was examined by Liew et al. (Liew, Kitipornchai, Leung, & Lim, 2003). They used the Ritz method for the formulation. Free vibration analysis of plate having rectangular shape using a finite element method was studied by Ramu and Mohanty (Ramu & Mohanty, 2012). Free vibration analysis of isotropic rectangular plates carrying a concentrated mass has been investigated by Boay (Boay, 1995). He incorporated Ritz method and presented the effect of non-dimensional frequency due to different locations of the concentrated mass on a plate. Ciancio et al. (Ciancio, Rossit, & Laura, 2007) carried out vibrational analysis of a cantilever anisotropic plate subjected to concentrated mass at the free end. They used Ritz method for the analysis and presented the variation of frequency due to variation of mass ratio and aspect ratio. Yu (Yu, 2009) carried out a study on free and forced vibration of cantilever plates subjected to point mass. He used Gorman's method of superposition for vibration analysis. and presented the variation of results for different aspect ratios. Dynamic analysis of laminated cylindrical shells (Jin, Ye, Chen, Su, & Yan, 2013), laminated plates (Ye, Jin, Su, & Chen, 2014), composite cylindrical shells with general elastic boundary conditions (Jin, et al., 2013), functionally graded cylindrical shells (Jin, Xie, & Liu, 2014), composite laminated structure elements of revolution (Jin, Ye, Jia, & Gao, 2014) has been carried out using an energy-oriented modified Fourier method.

The literature review reveals that there is a lacuna on the study of plates with arbitrary cut-outs carrying concentrated and distributed loads. In this paper, an attempt is made to tackle such interesting test cases using a highly accurate FSDT approach. Though newer and more accurate plate theories like higher-order shear deformation theory (HSDT) (Pandit, Sheikh, & Singh, 2010) (Chalak, Chakrabarti, Sheikh, & Iqbal, 2014), third-order shear deformation theory (TSDT) etc. exist, FSDT has been the choice of many researchers due to its computationally inexpensive nature. FSDT has been used from applications ranging from isotropic plates/shells (Kalita & Haldar, 2017) to composites (Lair, Hui, Sofiyev, Gribniak, & Turan, 2019) (Najafov, et al., 2014) (Sofiyev, 2018a) to functionally graded structures (Sofiyev, 2018b) (Haciyev, Sofiyev, & Kuruoglu, 2018) (Orakdöğen et al., 2010).

In the current work, the numerical analyses are carried out by developing a finite element model considering a nine-node isoparametric element. The paper begins with a general introduction to the problem and its scope. The second section details the finite element formulation along with the FSDT theory considered in this paper. The third section begins with benchmarking the current formulation with existing FSDT solutions. Further, in a novel attempt, certain interesting test cases relating to arbitrary positions of cut-outs, plates with cut-outs carrying concentrated mass, plates carrying distributed mass are studied. A concise conclusion of the work is presented in the final section of the manuscript.

2. FINITE ELEMENT FORMULATION

In this study, a nine-node isoparametric element is used in the current finite element formulation. One of the main advantages of the element is that any form of the plate can be well managed with an elegant mapping technique that can be defined as

$$x = \sum_{r=1}^9 N_r x_r \text{ and } y = \sum_{r=1}^9 N_r y_r \tag{1}$$

Thus, by using this simple mapping technique the coordinates at any place within the element (x, y) are expressed as the summation of the product of the Lagrange interpolation function (N_r) and the coordinates of the rth nodal point (x_r, y_r). Considering the bending rotations as independent field variables (since they are not derivatives of w), the effect of shear deformation may be incorporated as

$$\begin{Bmatrix} \phi_x \\ \phi_y \end{Bmatrix} = \begin{Bmatrix} \theta_x - \frac{\partial w}{\partial x} \\ \theta_y - \frac{\partial w}{\partial y} \end{Bmatrix}$$

Since this is an isoparametric formulation, the same interpolation functions are used for element geometry that have been used to describe the displacement field

$$\begin{aligned} w &= \sum_{r=1}^9 N_r w_r \\ \theta_x &= \sum_{r=1}^9 N_r \theta_{xr} \\ \theta_y &= \sum_{r=1}^9 N_r \theta_{yr} \end{aligned} \tag{2}$$

The stresses and strains of any continuous elastic material are connected by a linear relationship that is mathematically similar to Hooke's law and may be expressed as

$$\{\sigma\} = [D]\{\varepsilon\} \tag{3}$$

Where,

$$\{\sigma\} = [M_x \quad M_y \quad M_{xy} \quad Q_x \quad Q_y] \tag{4}$$

$$\{\varepsilon\} = \begin{Bmatrix} -\partial\theta_x/\partial x \\ -\partial\theta_y/\partial y \\ -\partial\theta_x/\partial y - \partial\theta_y/\partial x \\ \partial w/\partial x - \theta_x \\ \partial w/\partial y - \theta_y \end{Bmatrix} \tag{5}$$

$$[D] = \begin{bmatrix} D_{11} & D_{12} & 0 & 0 & 0 \\ D_{21} & D_{22} & 0 & 0 & 0 \\ 0 & 0 & D_{33} & 0 & 0 \\ 0 & 0 & 0 & D_{44} & 0 \\ 0 & 0 & 0 & 0 & D_{55} \end{bmatrix} \tag{6}$$

Where,

$$D_{11} = D_{22} = \frac{Eh^3}{12(1-\nu^2)}$$

$$D_{12} = D_{21} = \nu D_{11} = \nu D_{22}$$

$$D_{33} = \left(\frac{1-\nu}{2}\right) D_{11}$$

$$D_{44} = D_{55} = \frac{khE}{2(1+\nu)}$$

Here, k is the shear correction factor.

From Eqns. (2) and (5) the strain vector may be expressed as

$$\{\varepsilon\} = \sum_{r=1}^9 [B]_r \{\delta_r\}_e \tag{7}$$

$[B]$ is the strain-displacement matrix containing interpolation functions and their derivatives.

Using the virtual work method, the stiffness may be expressed as

$$[K] = h \int_{-1}^{+1} \int_{-1}^{+1} [B]^T [D] [B] |J| d\xi d\eta \tag{8}$$

where $|J|$ is the determinant of the Jacobian matrix.

Applying the concept of consistent mass matrix, a lumped mass matrix has been derived and it may be expressed as

$$[M] = \rho h \int_{-1}^{+1} \int_{-1}^{+1} \left[[N_u]^T [N_u] + [N_v]^T [N_v] + [N_w]^T [N_w] + \frac{h^2}{12} [N_{\theta_x}]^T [N_{\theta_x}] + \frac{h^2}{12} [N_{\theta_y}]^T [N_{\theta_y}] \right] |J| d\xi d\eta \tag{9}$$

The global stiffness matrix $[K_0]$ and global mass matrix $[M_0]$ are calculated by assembling individual stiffness matrix and the individual mass matrices of all the elements. Using the equation of motion, we get,

$$[K_0] = \omega^2 [M_0] \tag{10}$$

The calculated frequencies are presented in non-dimensional form $\lambda = \omega a^2 \sqrt{\rho h / D}$ where $D = \frac{Eh^3}{12(1-\nu^2)}$.

Table 1: Non-dimensional frequency parameter $\lambda = \omega a^2 \sqrt{\frac{\rho h}{D}}$ for simply supported square plate having different thickness ratio and mass lumping system. ($\nu = 0.3$).

h/a	Mass Lumping	Modes					
		1	2	3	4	5	6
0.01	LSWORI (8×8) ¹	19.733	49.321	49.321	78.849	98.696	98.696
	LSWORI (10×10)	19.734	49.316	49.316	78.860	98.614	98.614
	LSWORI (12×12)	19.734	49.315	49.315	78.864	98.585	98.585
	LSWORI (16×16)	19.734	49.314	49.314	78.867	98.566	98.567

3. RESULTS AND DISCUSSION

To exhibit the accuracy and applicability of the present formulation, few examples are studied in this section to show how the cut-out and its size affect to the natural frequencies of an isotopic plate having different boundary condition, different aspect ratio and thickness ratio. A finite element formulation is written in FORTRAN language.

3.1 CONVERGENCE AND VALIDATION STUDY

Example 1: A square plate with simply supported boundary condition having different thickness ratios and mass lumping schemes.

A simply supported (SSSS) square plate having different thickness ratios (h/a) is considered. Vibration due to two different mass lumping schemes is studied. In one mass lumping formulation rotary inertia is considered. The effect on non-dimensional frequencies due to rotary inertia and without rotary inertia are presented in Table 1 and also convergence study of the present formulation is presented. The solution converges at a mesh division of 20×20. Non-dimensional frequencies decrease when mass lumping with rotary inertia is considered. The effect of rotary inertia is less for thin plates and more in thick plates. Results obtained considering rotary inertia are very close to the closed-form solutions of Mindlin (Mindlin, 1951) for thin as well as thick plates.

Example 2: Simply supported square plate with central cut-out having different cut-out size.

A simply supported square plate as shown in Figure 1 with a thickness ratio $h/a = 0.01$ is considered. A central square cut-out having different cut-out size is considered for the analysis. The non-dimensional fundamental frequency obtained using the present formulation is shown in Figure 1 with that of Zhang et al. (Zhang, Wang, Pedroso, & Zhang, 2018). Zhang et al. analyzed the problem using Hencky bar-net model. As cut-out size increased stiffness decreases more compared to the reduction of mass of the plate up to a certain size of the cut-out ($c=0.2a$). After this as cut-out size increases, stiffness increases more compared to the reduction of mass of the plate. The present results are very close to those of Zhang et al.

	LSWORI (20×20)	19.734	49.314	49.314	78.868	98.561	98.562
	% Variation ²	-0.010	-0.022	-0.022	-0.033	-0.045	-0.046
	LSWRI (8×8)	19.731	49.311	49.311	78.823	98.656	98.656
	LSWRI (10×10)	19.732	49.306	49.306	78.834	98.574	98.574
	LSWRI (12×12)	19.732	49.305	49.305	78.838	98.545	98.545
	LSWRI (16×16)	19.732	49.304	49.304	78.842	98.526	98.526
	LSWRI (20×20)	19.732	49.304	49.304	78.842	98.521	98.521
	Mindlin (Mindlin, 1951)	19.732	49.303	49.303	78.842	98.517	98.517
	% Variation ³	0	-0.002	-0.002	0.000	-0.004	-0.004
0.1	LSWORI (12×12)	19.205	46.200	46.200	71.316	87.184	87.184
	LSWORI (16×16)	19.205	46.199	46.199	71.319	87.174	87.175
	LSWORI (20×20)	19.205	46.199	46.199	71.321	87.170	87.175
	% Variation	-0.734	-1.576	-1.576	-2.188	-2.507	-2.513
	LSWRI (12×12)	19.065	45.483	45.483	69.789	85.052	85.052
	LSWRI (16×16)	19.065	45.483	45.483	69.793	85.043	85.044
	LSWRI (20×20)	19.065	45.483	45.483	69.794	85.040	85.042
	Mindlin (Mindlin, 1951)	19.065	45.482	45.482	69.794	85.038	85.038
	% Variation	0.000	-0.002	-0.002	0.014	-0.002	-0.005
0.2	LSWORI (12×12)	17.830	39.460	39.460	57.242	64.385	64.385
	LSWORI (16×16)	17.830	39.460	39.460	57.246	64.385	64.385
	LSWORI (20×20)	17.830	39.460	39.460	57.248	64.388	64.388
	% Variation	-2.189	-3.428	-3.428	-3.804	1.162	1.162
	LSWRI (12×12)	17.449	38.152	38.152	55.146	64.384	64.384
	LSWRI (16×16)	17.449	38.152	38.152	55.150	64.387	64.387
	LSWRI (20×20)	17.449	38.152	38.152	55.154	64.388	64.388
	Mindlin (Mindlin, 1951)	17.448	38.152	38.152	55.150	65.145	65.145
	% Variation	-0.006	0.000	0.000	-0.007	1.162	1.162

¹ Number within the bracket represents mesh division of the plate.

² represents % error of present work without rotary inertia with respect to the literature.

³ represents % error of present work with rotary inertia with respect to the literature

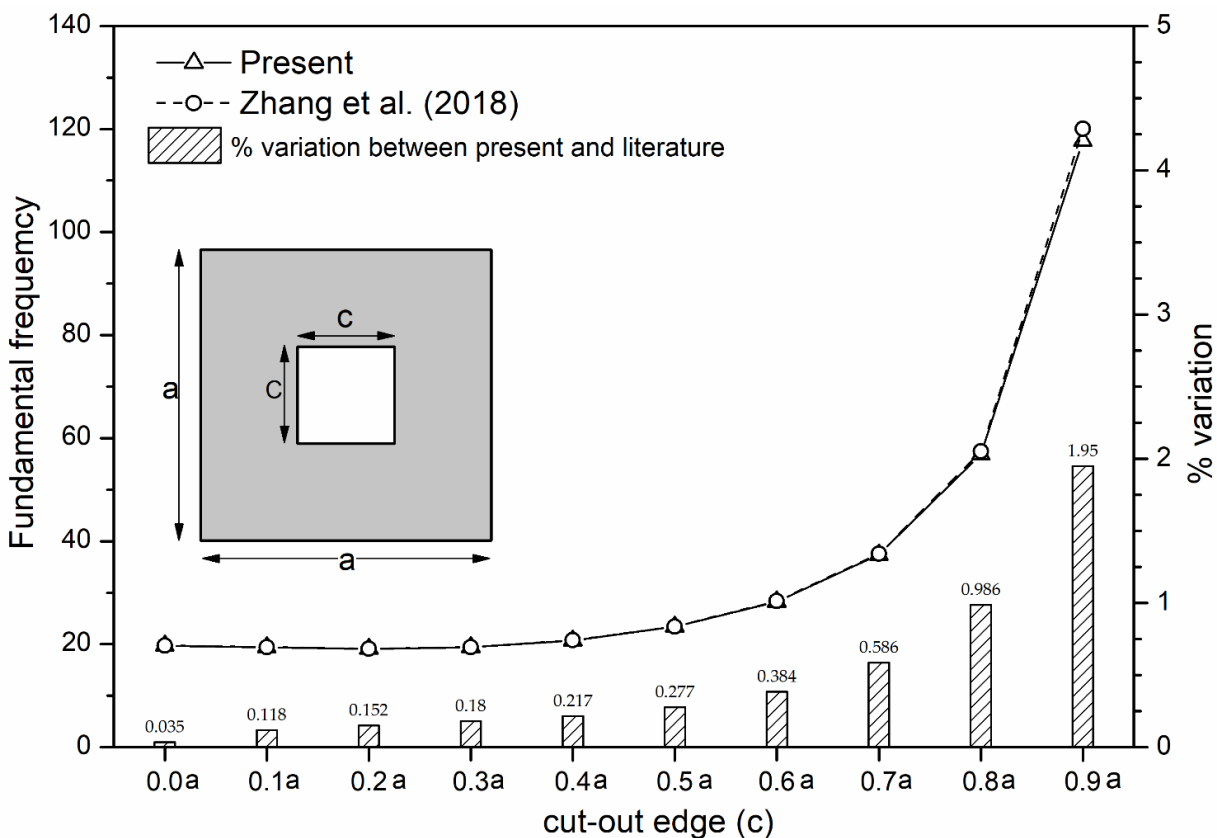


Figure. 1: Fundamental frequency of simply supported square plate with central cut-out having different cut-out size.

Example 3: Cut-out square plate having different boundary condition.

A square plate with a central square cut-out (0.4a×0.4b) having a ratio of thickness h/a=0.01 is considered. Here the boundary condition is applied at the outer edges as well as at the cut-out edges of the plate. A plate may have a combination of clamped (C), simply supported(S), and free (F) boundary conditions at the edges. Boundary condition CCSS-CCCC means, first boundary condition

CCSS for the outer edges of the plate and second one, CCCC for the cut-out edges. Boundary condition CCSS means plate is clamped at $x = 0$ and $x = a$, simply supported at $y = a$ and $y = 0$. Non-dimensional frequencies in different boundary conditions are presented in Table 2 and the percentage variation in results with Zhang et al. (Zhang, Wang, Pedroso, & Zhang, 2018) are also presented. There is good agreement between the present results with that of Zhang et al. (Zhang, Wang, Pedroso, & Zhang, 2018).

Table 2: Non-dimensional frequency parameter $\lambda = \omega a^2 \sqrt{\frac{\rho h}{D}}$ for square plate with central square cut-out (0.4a×0.4b) having different boundary conditions at outer and inner cut-out edges of the plate. ($h/a = 0.01, \nu = 0.3$).

Modes	Present	Zhang et al. (2018)	% Variation	Present	Zhang et al. (2018)	% Variation	Present	Zhang et al. (2018)	% Variation
Boundary Condition									
1	49.196	49.303	0.22	20.708	20.752	0.21	35.48	35.562	0.23
2	65.459	65.954	0.75	40.719	41.039	0.78	46.079	46.467	0.84
3	65.459	65.954	0.75	40.719	41.039	0.78	61.52	61.929	0.66
4	98.965	99.419	0.46	71.166	71.355	0.26	86.101	86.419	0.37
5	104.76	106.22	1.37	81.631	82.488	1.04	94.345	95.45	1.16
Boundary Condition									
1	223.247	223.39	0.06	185.64	187.93	1.22	150.49	150.29	-0.13
2	224.451	224.63	0.08	189.98	190.2	0.12	152.62	152.4	-0.14
3	224.451	224.63	0.08	189.98	190.2	0.12	152.62	152.4	-0.14
4	225.91	226.18	0.12	195.13	194.84	-0.15	155.58	155.38	-0.13
5	260.69	260.71	0.01	211.49	208.64	-1.37	185.18	185.43	0.13
Boundary Condition									
1	122.06	124.91	2.28	170.762	170.7	-0.04	131.25	132.73	1.12
2	127.21	127.98	0.6	170.8	170.72	-0.05	132.1	132.74	0.48
3	127.21	127.98	0.6	184.24	184.25	0.01	168.99	168.9	-0.05
4	135.85	135.76	-0.07	184.3	184.27	-0.02	171.44	169.61	-1.08
5	145.81	144.11	-1.18	223.024	223.45	0.19	186.62	187.8	0.63

Example 4: Cantilever plate carrying concentrated mass at the edge.

A plate with side (a) and width (b) as shown in Figure 2 is considered. Boundary condition applied on the plate is CFFF, which means clamped at $x = 0$ and other edges $x = a, y = a, y = 0$ are free. A point mass is applied at the point (a, 0.5b). Variation of the non-dimensional frequency with variation of aspect ratio is shown in Table 3. Present results are compared with Yu (Yu, 2009) and percentage variations are also presented. Present results are very accurate and closed to Yu (Yu, 2009).

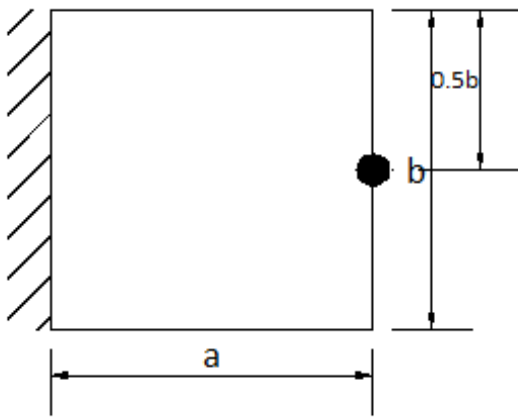


Figure 2: Cantilever plate with point mass at the edge.

Table 3: Non-dimensional frequency $\lambda = \omega a^2 \sqrt{\frac{\rho h}{D}}$ for rectangular cantilever plate carrying concentrated mass at the edge. ($M_c/M_p = 0.5, h/b = 0.01, \nu = 0.3$).

b/a	Source	Modes				
		1	2	3	4	5
2.0	Present	1.881	7.163	17.17	23.89	33.64
	Yu (Yu, 2009)	1.886	7.218	17.36	24.09	33.83
	% Variation	0.27	0.76	1.09	0.83	0.56
1.0	Present	1.960	13.66	25.66	40.68	59.77
	Yu (Yu, 2009)	1.962	13.72	25.71	41.03	59.92
	% Variation	0.10	0.44	0.19	0.85	0.25
0.5	Present	1.962	16.04	45.78	78.59	105.2
	Yu (Yu, 2009)	1.964	16.08	45.96	78.83	105.5
	% Variation	0.10	0.25	0.39	0.30	0.28

3.2 NUMERICAL RESULTS

3.2 (a) Rectangular plate with central cut-out having different thickness ratio and mass lumping schemes

A square plate with a central cut-out (0.4ax0.4b) is considered. The analysis is performed using both the mass lumping schemes. The variation of non-dimensional frequency with variation of thickness ratio, for different mass lumping schemes is shown in Table 4. From Table 4 we can find that non-dimensional frequencies decrease as the ratio of thickness increases from 0.01 to 0.2 and non-dimensional frequencies decrease when lumping schemes with rotary inertia is in consideration. Effect of rotary inertia is negligible when the thickness ratio is small (0.01) but with an increase of thickness ratio, frequency changes due to rotary inertia.

3.2 (b) Rectangular plate with central cut-out having different side ratio

A rectangular plate with a central cut-out (0.4ax0.4b) having thickness ratio $h/b = 0.01$ is considered. Non-dimensional frequencies with variation of aspect ratio in different boundary conditions are presented in Table 5. As aspect ratio increases, both stiffness and mass of the plate increase. But here stiffness is more predominant compared to the effect of the mass of the plate. Therefore, non-dimensional frequencies are increased as the aspect ratio of the plate is increased.

3.2 (c) Rectangular plate with cut-out

The square plate as shown in Figure 3 with a cut-out (c x d) is considered. Effect on non-dimensional frequencies due to change in cut-out size and thickness ratio in different conditions of boundary is presented in Table 6. It is clear from Table 6 that non-dimensional frequencies decreased as the thickness ratio of the plate is increased which is expected because of increase of mass. On the other hand, non-dimensional frequency increases when the length of the cut-out (c) is increased due to the decrease of mass of the plate.

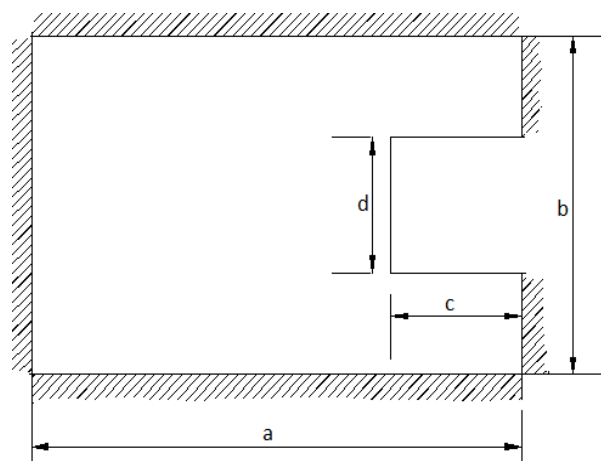


Figure 3: Rectangular plate with cut-out

Table 4: Non-dimensional frequency $\lambda = \omega a^2 \sqrt{\frac{\rho h}{D}}$ for square plate with central square cut-out of (0.4a×0.4b) having different thickness ratio and boundary condition. ($a/b = 1, \nu = 0.3$).

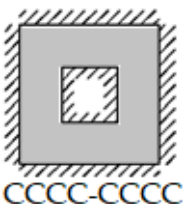
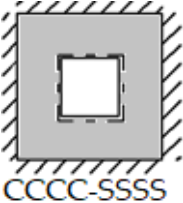
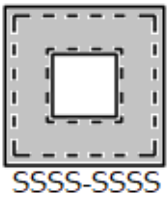
Boundary Condition	h/b	Modes						% difference		
		LSWRI			LSWORI			1	2	3
		1	2	3	1	2	3			
 CCCC-CCCC	0.01	223.247	224.451	224.451	223.369	224.578	224.578	0.055	0.057	0.057
	0.1	139.269	139.786	139.786	140.763	141.553	141.553	1.061	1.248	1.248
	0.2	84.253	85.016	85.017	84.791	85.932	85.933	0.635	1.066	1.066
 CCCC-SSSS	0.01	185.642	189.978	189.978	185.742	190.086	190.086	0.054	0.057	0.057
	0.1	122.529	125.375	125.375	124.515	127.536	127.536	1.595	1.694	1.694
	0.2	78.325	80.118	80.118	79.718	81.719	81.719	1.747	1.959	1.959
 SSSS-SSSS	0.01	150.492	152.617	152.617	150.565	152.694	152.694	0.048	0.050	0.050
	0.1	108.334	109.973	109.973	110.546	112.365	112.365	2.001	2.129	2.129
	0.2	70.844	71.417	73.296	70.844	73.788	74.865	0.000	3.213	2.096

Table 5: Non-dimensional frequency $\lambda = \omega a^2 \sqrt{\frac{\rho h}{D}}$ for square plate with central square cut-out of (0.4a×0.4b) having different aspect ratio and different boundary condition. ($h/b = 0.01, \nu = 0.3$).


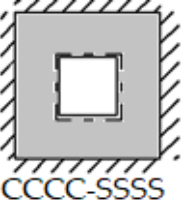

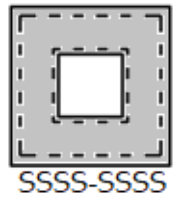
a/b	Boundary Condition	Modes			Boundary Condition	Modes		
		1	2	3		1	2	3
1.0	 CCCC-CCCC	223.247	224.451	224.451	 CCCC-SSSS	185.642	189.978	189.978
1.5		262.486	262.542	310.445		212.108	212.811	293.348
2.0		285.509	285.525	402.633		240.841	241.093	389.552
3.0		361.598	361.624	684.194		329.756	330.180	677.054
1.0	 SSSS-CCCC	150.492	152.617	152.617	 SSSS-SSSS	122.060	127.209	127.209
1.5		180.862	180.923	221.734		145.261	146.349	209.709
2.0		197.763	197.798	291.262		165.253	165.897	281.501
3.0		241.545	241.576	483.656		215.544	215.968	477.028

Table 6: Non-dimensional frequency $\lambda = \omega a^2 \sqrt{\frac{\rho h}{D}}$ for a square plate with rectangular cut-outs ($c \times d$) having different thickness ratio and different boundary condition. ($a/b = 1, \nu = 0.3$)

Boundary Condition										
Cut-out size ($c \times d$)	h/b	Modes								
		1	2	3	1	2	3	1	2	3
0.4a×0.6b	0.01	31.780	71.560	79.488	17.867	45.253	56.194	23.223	49.793	72.960
	0.1	28.228	60.544	66.172	16.716	41.483	50.265	20.944	44.506	55.101
	0.2	23.158	45.491	48.883	14.945	25.133	28.178	17.752	27.551	36.207
0.6a×0.6b	0.01	42.554	81.206	111.883	21.165	42.612	57.224	32.138	49.432	67.628
	0.1	36.930	67.590	87.968	19.742	38.168	45.592	28.918	42.698	54.533
	0.2	29.611	50.233	62.932	17.526	22.796	27.290	23.942	31.683	33.284
0.8a×0.6b	0.01	96.925	100.930	109.298	29.906	37.655	52.119	45.242	45.512	91.169
	0.1	79.331	81.472	85.947	27.361	32.964	33.121	37.882	37.941	56.381
	0.2	58.031	59.302	61.844	16.560	21.421	23.313	28.191	28.364	28.480

Table 7: Non-dimensional frequency $\lambda = \omega a^2 \sqrt{\frac{\rho h}{D}}$ for a rectangular plate with cut-out ($c \times d$) having different aspect ratio and different boundary condition. ($h/b = 0.01, \nu = 0.3$)

Boundary Condition										
Cut-out size ($c \times d$)	a/b	Modes								
		1	2	3	1	2	3	1	2	3
0.6a×0.6b	1.0	42.554	81.206	111.883	21.165	42.612	57.224	32.138	49.432	67.628
	1.5	71.335	160.009	177.887	34.651	71.544	82.103	43.540	78.004	94.355
	2.0	111.413	215.714	269.262	51.720	99.786	106.057	59.081	107.155	119.065
	3.0	224.737	324.782	541.554	97.363	153.835	156.612	102.413	161.999	169.762
0.9a×0.6b	1.0	100.212	100.212	136.246	33.205	35.269	68.604	42.862	42.862	94.791
	1.5	208.538	208.557	241.620	48.944	52.064	95.935	58.573	58.583	123.524
	2.0	360.608	361.330	386.147	65.110	69.237	124.880	74.863	74.971	154.335
	3.0	522.758	796.599	800.211	98.259	104.143	186.315	107.855	108.803	217.695

Table 8: Non-dimensional frequency $\lambda = \omega a^2 \sqrt{\frac{\rho h}{D}}$ for rectangular plates with two cut-outs having different boundary condition. ($a/b = 2, h/b = 0.01, \nu = 0.3$)

Boundary Condition	Modes				
	1	2	3	4	5
	578.825 	602.657 	602.787 	612.821 	657.913
	398.264 	398.408 	454.184 	454.438 	491.610
	379.388 	475.503 	475.940 	566.657 	620.727
	491.616 	494.402 	552.370 	552.536 	564.502
	315.570 	316.368 	369.273 	425.578 	428.177
	369.340 	458.306 	462.201 	464.201 	490.549

Table 9: Non-dimensional frequency $\lambda = \omega a^2 \sqrt{\frac{\rho h}{D}}$ for a square cantilever plate with cut-out having same cut-out area. ($a/b = 1, h/b = 0.01, \nu = 0.3$)

Boundary Condition	Mode Number				
	1	2	3	4	5
	4.252 	6.350 	20.520 	22.967 	25.940
	4.216 	12.881 	20.306 	33.455 	39.990
	4.075 	12.307 	19.981 	27.115 	45.915

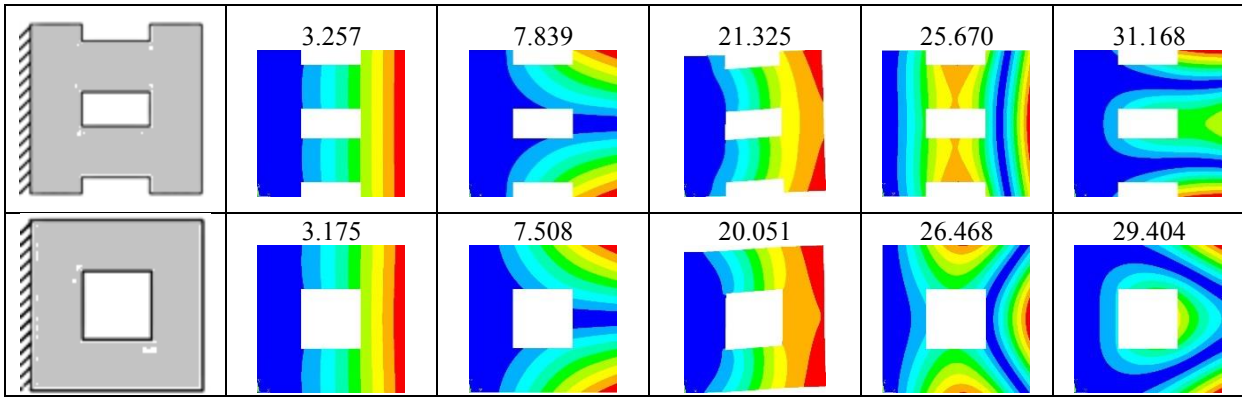


Table 10: Non-dimensional frequency $\lambda = \omega a^2 \sqrt{\frac{\rho h}{D}}$ for a rectangular plate with cut-out having concentrated mass. ($a/b = 1, h/b = 0.01, \nu = 0.3$)

Modes	Boundary Condition	M_c/M_p			Boundary Condition	M_c/M_p		
		1	0.75	0.5		1	0.75	0.5
1		4.075	4.079	4.095		1.443	1.616	1.871
2		10.911	12.307	12.307		7.839	7.839	7.839
3		12.307	12.599	15.43		13.372	13.653	14.168
4		19.981	19.981	19.981		23.509	23.524	23.555
5		27.115	27.115	27.115		31.168	31.168	31.168
1		1.619	1.827	2.143		1.647	1.857	2.176
2		12.881	12.881	12.881		2.288	2.59	3.054
3		14.294	14.47	14.795		14.945	15.116	15.43
4		33.455	33.455	33.455		17.427	17.574	17.848
5		37.635	37.756	37.973		25.349	25.358	25.376
1		1.404	1.572	1.82	Concentrated mass is equally distributed at both points			
2		7.508	7.508	7.508				
3		12.735	12.986	13.446				
4		25.686	25.701	25.729				
5		29.404	29.404	29.404				

Table 11: Non-dimensional frequency $\lambda = \omega a^2 \sqrt{\frac{\rho h}{D}}$ for a square plate carrying distributed mass (M_d) throughout the plate. ($a/b = 1, h/b = 0.01, \nu = 0.3$)

Boundary Condition	M_d/M_p	Modes					
		1	2	3	4	5	6
CCCC	1.0	25.728	52.429	52.429	77.238	93.884	94.34
	0.75	27.456	55.949	55.950	82.424	100.19	100.67
	0.5	29.586	60.290	60.290	88.818	107.96	108.48
SSSS	1.0	14.124	35.294	35.294	56.442	70.532	70.533
	0.75	15.073	37.664	37.664	60.232	75.268	75.268
	0.5	16.242	40.586	40.586	64.904	81.106	81.106
CCSS	1.0	20.704	39.137	49.534	67.552	73.029	92.129
	0.75	22.094	41.765	52.860	72.088	77.932	98.314
	0.5	23.809	45.005	56.961	77.679	83.964	105.94

Table 12: Non-dimensional frequency $\lambda = \omega a^2 \sqrt{\frac{\rho h}{D}}$ for a square cut-out plate(0.4a×0.4b) carrying distributed mass (M_d) throughout the plate. ($a/b = 1, h/b = 0.01, \nu = 0.3$)

Boundary Condition	M_d/M_p	Modes					
		1	2	3	4	5	6
CCCC	1.0	35.538	47.422	47.422	72.443	76.050	108.328
	0.75	37.875	50.518	50.518	77.054	80.994	115.182
	0.5	40.742	54.313	54.313	82.673	87.045	123.524
SSSS	1.0	15.098	29.781	29.781	52.481	59.857	86.404
	0.75	16.068	31.680	31.680	55.757	63.650	91.794
	0.5	17.253	33.995	33.995	59.735	68.269	98.337
CCSS	1.0	25.783	33.636	44.677	63.280	68.727	93.859
	0.75	27.454	35.791	47.578	67.266	73.155	99.762
	0.5	29.498	38.422	51.127	72.114	78.565	106.938

3.2 (d) Cut out rectangular plate

A rectangular plate as shown in Figure. 3 with a cut-out having thickness $h/b = 0.01$ is considered. The effect in non-dimensional frequencies due to change in cut-out size and side ratio in different boundary conditions are studied and presented in Table 7. Non-dimensional frequency increase as the side ratio of the plate is increased due to the increase of stiffness of the plate.

3.2 (e) Rectangular plate with two central cut-outs

A rectangular plate with two cut-outs having side ratio $a/b=2.0$ and ratio of thickness $h/b = 0.01$ as shown in Figure. 4 is considered. Variation in non-dimensional frequencies due to cut-out (0.2a×0.4b) and different boundary conditions are presented in Table 8 with the corresponding mode shapes. Boundary conditions are applied at the outer edges as well as along the edges of cut-outs.

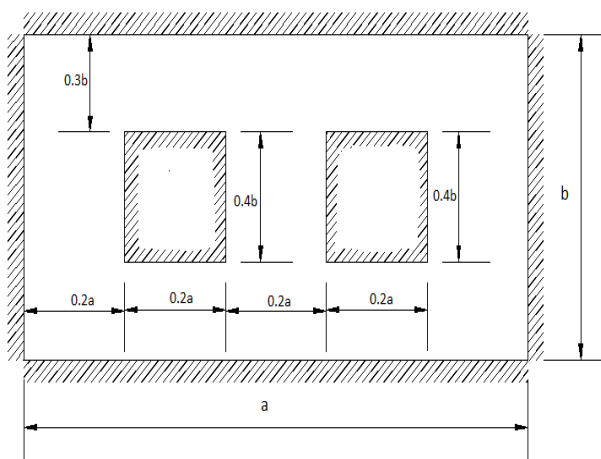


Figure 4: Rectangular plate with two internal cut-outs

3.2 (f) Cantilever plates with cut-out

A square cantilever plate having different position of the cut-outs is considered. The area of the cut-out is same for all the plates. It means that mass remains same for all the

plates. Variations of non-dimensional frequencies due to the variation of the position of cut-out are presented in Table 9. Corresponding mode shapes are also presented in the table. It is seen that cantilever plate having cut out at the centre has minimum frequencies as it has minimum stiffness.

3.2 (g) Cantilever plates with cut-out having concentrated mass at free edge.

A square plate with one edge fixed and other edges free having different position of the cut-out is considered. The area of the cut-out for every plate is the same. A point mass is applied at the free edge of the plate as shown in the figures in Table 10. Variations of non-dimensional frequencies due to different mass ratio, different position of applied mass are presented in Table 10. From Table 10, it is clear that non-dimensional frequencies increased when the mass ratio is decreased.

3.2 (h) Plates carrying distributed mass

A square plate subjected to uniform distributed mass is considered. Non-dimensional frequencies in different boundary conditions and for different mass distributions (M_d/M_p) are presented in Table 11. Non-dimensional frequencies increase when the intensity of distributed mass is decreased.

3.2 (i) Cut-out plates carrying distributed mass.

A square plate having central cut-out (0.4a×0.4b) subjected to uniformly distributed mass is considered. Non-dimensional frequencies for different boundary conditions and different mass distributions (M_d/M_p) are presented in Table 12. Non-dimensional frequencies increase when the intensity of distributed mass is decreased.

4. CONCLUSION

In this paper, a finite element formulation based on the 9-node isoparametric element is used for calculating the dynamic responses of plates with rectangular-shaped cut-

outs. Mindlin's theory is incorporated in the formulation to account for shear deformation. Further, the formulation is enhanced by using two different mass lumping schemes that allow the effect of rotary inertia to be included or excluded. Thus, the contribution and effect of rotary inertia can be accurately evaluated. It is seen that the average difference between fundamental frequencies calculated with and without rotary inertia is less than 1%. For higher frequencies, the difference is seen to be less than 2%. Based on the results it is seen that mass lumping with rotary inertia is suitable for both thin and thick plates whereas mass lumping without rotary inertia is only suitable for thin plates. The comparison of the calculated solutions with existing literature shows excellent conformity in results. After thorough validation and testing of the present finite element formulation, several interesting examples having rectangular shaped cut-outs at different positions, cut-out plates carrying concentrated mass and uniformly distributed mass are presented which will serve as benchmark solutions for upcoming works.

5. REFERENCES

1. ABBAS, E. N., ABDULLAH, M. Q. & WASMI, H. R., 2015. *Static & Free Vibration Analysis of an Isotropic and Orthotropic Thin Plate using Finite Element Analysis (FEA)*. International Journal of Current Engineering and Technology, Volume 5, pp. 462-468.
2. BOAY, C. G., 1995. *Frequency analysis of rectangular isotropic plates carrying a concentrated mass*. Computers & structures, Volume 56, pp. 39-48. DOI: 10.1016/0045-7949(94)00533-9
3. CHALAK, H. D., CHAKRABARTI, A., SHEIKH, A. H., & IQBAL, M. A., 2014. *C0 FE model based on HOZT for the analysis of laminated soft-core skew sandwich plates: Bending and vibration*. Applied Mathematical Modelling, Volume 38, pp. 1211-1223. DOI: 10.1016/j.apm.2013.08.005
4. CIANCIO, P. M., ROSSIT, C. A., & LAURA, P. A., 2007. *Approximate study of the free vibrations of a cantilever anisotropic plate carrying a concentrated mass*. Journal of Sound and Vibration, Volume 302, pp. 621-628. DOI: 10.1016/j.jsv.2006.11.027
5. CORR, R., & JENNINGS, A., 1976. *A simultaneous iteration algorithm for symmetric eigen value problems*. Int. J. Numer. Eng., Volume 10, pp. 647-663. DOI: 10.1002/nme.1620100313
6. HACIYEV, V. C., SOFIYEV, A. H., & KURUOGLU, N., 2018. *Free bending vibration analysis of thin bidirectionally exponentially graded orthotropic rectangular plates resting on two-parameter elastic foundations*. Composite Structures, Volume 184, pp. 372-377. DOI: 10.1016/j.compstruct.2017.10.014
7. JIN, G., XIE, X., & LIU, Z., 2014. *The Haar wavelet method for free vibration analysis of functionally graded cylindrical shells based on the shear deformation theory*. Composite Structures, Volume 108, pp. 435-448. DOI: 10.1016/j.compstruct.2013.09.044
8. JIN, G., YE, T., CHEN, Y., SU, Z., & YAN, Y., 2013. *An exact solution for the free vibration analysis of laminated composite cylindrical shells with general elastic boundary conditions*. Composite Structures, Volume 106, pp. 114-127. DOI: 10.1016/j.compstruct.2013.06.002
9. JIN, G., YE, T., JIA, X., & GAO, S., 2014. *A general Fourier solution for the vibration analysis of composite laminated structure elements of revolution with general elastic restraints*. Composite Structures, Volume 109, pp. 150-168. DOI: 10.1016/j.compstruct.2013.10.052
10. JIN, G., YE, T., MA, X., CHEN, Y., SU, Z., & XIE, X., 2013. *A unified approach for the vibration analysis of moderately thick composite laminated cylindrical shells with arbitrary boundary conditions*. International Journal of Mechanical Sciences, Volume 75, pp. 357-376. DOI: 10.1016/j.ijmecsci.2013.08.003
11. KALITA, K., & HALDAR, S., 2016. *Free vibration analysis of rectangular plates with central cutout*. Cogent Engineering, Volume 3, 1163781. DOI: 10.1080/23311916.2016.1163781
12. KALITA, K., & HALDAR, S., 2017. *Eigenfrequencies of simply supported taper plates with cut-outs*. Structural Engineering and Mechanics, Volume 63, pp. 103-113.
13. LAIR, J., HUI, D., SOFIYEV, A. H., GRIBNIAK, V., & TURAN, F., 2019. *On the parametric instability of multilayered conical shells using the FOSDT*. Steel and Composite Structures, Volume 31, pp. 277-290.
14. LAM, K. Y., HUNG, K. C., & CHOW, S. T., 1989. *Vibration analysis of plates with cutouts by the modified Rayleigh-Ritz method*. Applied Acoustics, Volume 28, pp. 49-60. DOI: 10.1016/0003-682X(89)90030-3
15. LIEW, K. M., KITIPORNCHAI, S., LEUNG, A. Y., & LIM, C. W., 2003. *Analysis of the free vibration of rectangular plates with central cut-outs using the discrete Ritz method*. International journal of mechanical sciences, Volume 45, pp. 941-959. DOI: 10.1016/S0020-7403(03)00109-7
16. MANNA, M. C., 2005. *Free vibration analysis of isotropic rectangular plates using a high-order triangular finite element with shear*. Journal of sound and vibration, Volume 281, pp. 235-259. DOI: 10.1016/j.jsv.2004.01.015
17. MINDLIN, R. D., 1951. *Influence of rotatory inertia and shear on flexural motions of isotropic, elastic plates*. J. appl. Mech., Volume 18, pp. 31-38.

18. NAJAFOV, A. M., SOFIYEV, A. H., HUI, D., KARACA, Z., KALPAKCI, V., & OZCELIK, M., 2014. *Stability of EG cylindrical shells with shear stresses on a Pasternak foundation*. Steel and Composite Structures, Volume 17, pp. 453-470. DOI: 10.12989/scs.2014.17.4.453
19. ORAKDÖĞEN, E., KÜÇÜKARSLAN, S., SOFIYEV, A., & OMURTAG, M. H., 2010. *Finite element analysis of functionally graded plates for coupling effect of extension and bending*. Meccanica, Volume 45(1), pp. 63-72. DOI: 10.1007/s11012-009-9225-z
20. PANDIT, M. K., HALDAR, S., & MUKHOPADHYAY, M., 2007. *Free vibration analysis of laminated composite rectangular plate using finite element method*. Journal of Reinforced Plastics and Composites, Volume 26, pp. 69-80. DOI: 10.1177/0731684407069955
21. PANDIT, M. K., SHEIKH, A. H., & SINGH, B. N., 2010. *Analysis of laminated sandwich plates based on an improved higher order zigzag theory*. Journal of Sandwich Structures & Materials, Volume 12, pp. 307-326. DOI: 10.1177/1099636209104517
22. PARK, M., & CHOI, D.-H., 2018. *A two-variable first-order shear deformation theory considering in-plane rotation for bending, buckling and free vibration analyses of isotropic plates*. Applied Mathematical Modelling, Volume 61, pp. 49-71. DOI: 10.1016/j.apm.2018.03.036
23. RAMU, I., & MOHANTY, S. C., 2012. *Study on free vibration analysis of rectangular plate structures using finite element method*. Procedia engineering, Volume 38, pp. 2758-2766. DOI: 10.1016/j.proeng.2012.06.323
24. SOFIYEV, A. H., 2018a. *Application of the first order shear deformation theory to the solution of free vibration problem for laminated conical shells*. Composite Structures, Volume 188, pp. 340-346. DOI: 10.1016/j.compstruct.2018.01.016
25. SOFIYEV, A. H., 2018b. *Application of the FOSDT to the solution of buckling problem of FGM sandwich conical shells under hydrostatic pressure*. Composites Part B: Engineering, Volume 144, pp. 88-98. DOI: 10.1016/j.compositesb.2018.01.025
26. YE, T., JIN, G., SU, Z., & CHEN, Y., 2014. *A modified Fourier solution for vibration analysis of moderately thick laminated plates with general boundary restraints and internal line supports*. International Journal of Mechanical Sciences, Volume 80, pp. 29-46. DOI: 10.1016/j.ijmecsci.2014.01.001
27. YU, S. D., 2009. *Free and forced flexural vibration analysis of cantilever plates with attached point mass*. Journal of sound and vibration, 321, pp. 270-285. DOI: 10.1016/j.jsv.2008.09.042
28. ZHANG, Y. P., WANG, C. M., PEDROSO, D. M., & ZHANG, H., 2018. *Extension of Hencky bar-net model for vibration analysis of rectangular plates with rectangular cutouts*. Journal of Sound and Vibration, Volume 432, pp. 65-87. DOI: 10.1016/j.jsv.2018.06.0